2nd MCRC International Conference on Mobile and Personal Communications Systems
10–11 April 1995, Adelaide, Australia

Interference Modelling and Outage Contours in Cellular and Microcellular Networks

Brendan C. Jones and David J. Skellern

Electronics Department
School of Maths, Physics, Computing and Electronics
Macquarie University NSW 2109 Australia

email: brendan@mpce.mq.edu.au, daves@mpce.mq.edu.au

Abstract

This paper presents an interference model for cellular and microcellular networks. This model enables a unified treatment of all reception environments from purely noise limited to purely interference limited through a parameter denoted the 'interference to noise ratio' or INR.

Using the model, a simplified spatial description of mobile link outage contours is derived. Computer simulations are used to test the analytical theory. It is shown that as a link becomes more interference limited, larger variations in cell sizes result.

0 Introduction

The concept of cellular telecommunications was developed by the Bell Telephone Laboratories in the early 1970's [1]. Cellular or large cell systems use fixed channel allocations (FCA) that enable a receiver at a cell boundary to meet the signal to interference ratio (S/I) required for good signal quality in the presence of cochannel interferers [2]–[6].

The capacity of cellular systems can be increased by splitting existing cells but in practice there are limitations to the extent to which cells can be physically reduced in size. The limit for most large cell systems appears to be a cell radius of approximately 1 kilometre.

To meet the demands of the vision of a personal communicator in every pocket, a new architecture was required. Microcellular architecture differs from conventional or large cell architecture in three fundamental ways:

- The cells are typically less than 1 km in radius
- The mobile terminals radiate much smaller power levels
- There is no centralised, fixed cell planning (all channels are available in every cell)

The aims of a future Personal Communications Service (PCS) provided by such a ubiquitous microcell network include [7]:

- Low cochannel interference (< 1% of users)
- Closer frequency reuse
- Large percentage coverage (> 99%)

Interference in microcells is controlled at the time of call establishment by making interference measurements to find the 'best channel', a procedure called Dynamic Channel Allocation (DCA). Also, interference is reduced by having a smaller transmitter power than used in large cell systems, and sometimes further reduced by varying the transmitter power during the call to the minimum necessary [8].

However, the wide scale deployment of such an extensive, high grade, wireless telephone system will require engineering tools and techniques that allow rapid and accurate system design, and the fundamental problem that needs to be addressed is of modelling the end result of multiple users propagating in a congested area [9],[10].

1 System Design Issues

There does not yet appear to be a systematic design methodology for engineering a microcellular network to a target service quality [9]–[12]. Consideration of service quality as part of the system design is an imperative

because as the user base increases, people will no longer accept poor call quality simply because the service is 'mobile' [12] but will demand a similar grade of service to that experienced in wireline services [9].

The applicability of conventional cellular design techniques to the microcellular case is questionable. Firstly, the regular hexagonal structures that can be applied to large cell systems lead to a simple relationship between the cluster size *C* and the S/I, but no such simple relationship for *C* exists in microcells [13]. Microcells often overlap and become irregular in shape due to interference from other users [14] despite the use of DCA and/or power control because these techniques can still fail under heavy traffic loads [15].

Secondly, assumptions that only the first cochannel tier of interferers dominates in a large cell system [5] may not be applicable in microcell systems [16]. Also, it has been shown that adjacent channel interference (ACI) can affect the performance of heavily loaded systems [17]–[19]. In practical systems with non-uniform cells and unknown mobile positions, the effects of ACI and further off–channel interference could be even worse [16].

Thirdly, the close spacing of base stations in microcellular systems (especially in multioperator environments) and higher frequency reuse have a very significant impact upon the percentage of service area that has a circuit quality better than some specified value [7],[20],[21]. The impact of spatial traffic variability also needs to be considered [14],[20],[22].

These factors may make it very difficult to engineer a microcell system so that reliable, contiguous radio coverage is achieved. It has been suggested that contiguous coverage may be impossible to achieve [23],[24].

To move forward, a model is needed that can describe the cumulative interference effects of all users in an arbitrary cellular network, and that enables a uniform analysis from noise to interference limited environments. Both thermal noise and propagated interference need to be considered because the transmission quality is strongly dependent upon these two factors [25].

2 Basic Interference Model

The first step is to examine the fundamental effects of a single interferer on the useful range of a radio link. A common measure of link quality is the Signal to Noise ratio (S/N) or Signal to Noise plus Interference ratio (S/[N+I]). Where a link cannot be maintained at a desired quality due to insufficient S/[N+I] an 'outage' occurs. The region in which this threshold is maintained is the region in which radiocommunication is considered successful and is called the 'cell'.

2.1 Single Interferer – Interference Only

An analysis of link outage in the presence of an interferer but in the absence of receiver noise was presented in [26]. Consider the scenario in figure 1, where a mobile station M_0 is attempting communication with a fixed station F_0 at a range R_0 in the presence of a single interferer F_j which is at a range R_j from M_0 and a range S from F_0.

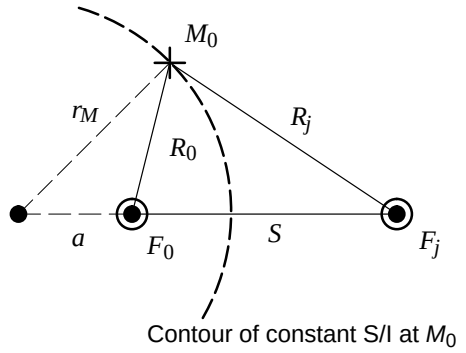

Figure 1 – A mobile link operating in the presence of an interferer

M_0 and F_0 transmit the wanted duplex signal at a power P_t. The interferer F_j spills an interference power P_u into the wanted uplink (M_0 to F_0) and P_d into the wanted downlink (F_0 to M_0).

The analysis in [26] was based upon a simple distance–dependent propagation model for analytical tractability:

$$P_{rx} = \kappa P_{tx} d^{-\gamma} \quad (1)$$

where P_{tx} is the transmitted power, P_{rx} is the average power received at a distance d from the transmitter and κ is an RF factor. The exponent γ is called the path loss exponent and represents how quickly the average received power falls away with distance. In free space $\gamma = 2$ and in a cluttered environment $\gamma > 2$.

In order for the mobile F_0 to successfully establish a link with M_0, the S/I at M_0 needs to be greater than or equal to the system protection ratio Z. If the fixed station F_0 is at the origin of the Cartesian plane, F_j is at $(S,0)$ and the mobile M_0 is at (x,y) it was shown in [26] that the outage contour (the locus where S/I = Z) at the *mobile* end of the link is a family of circles with centres (a,b) and radii r_M of:

$$(a,b) = \left(\frac{SK_d^{2/\gamma}}{K_d^{2/\gamma} - 1}, 0 \right) \quad (2)$$

$$r_M = \frac{SK_d^{1/\gamma}}{\left| 1 - K_d^{2/\gamma} \right|} \quad (3)$$

The parameter K is given by [26]:

$$K = \frac{P_t G_r W_j L_s}{Z P_j W_b} \quad (4)$$

where G_r is the net antenna gain between the interferer and receiver, L_s is a system loss factor, P_j is the interference power, and W_j and W_b are the bandwidths of the interfering and wanted signals respectively. If these bandwidths are equal and G_r and L_s are unity, the expression simplifies to $K_d = P_t/ZP_d$ for the downlink and $K_u = P_t/ZP_u$ for the uplink.

The resultant family of outage contours at the mobile end of the link is shown in figure 2. In the case of $K_d^{2/\gamma} = 1$ the mobile end outage contour degenerates to an infinite line perpendicular to, and at the midpoint of, the line joining F_0 with F_j. The region of link closure is within the contours for $K_d^{2/\gamma} < 1$, to the left of the contour for $K_d^{2/\gamma} = 1$, and to the exterior of the contours for $K_d^{2/\gamma} > 1$.

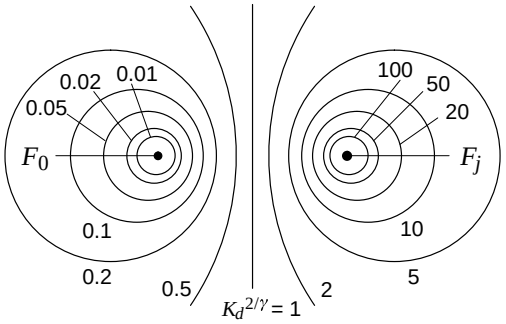

Figure 2 – Single interferer mobile end outage contours versus $K_d^{2/\gamma}$

At the *fixed* end of the link, it was shown in [26] that the outage contour is a family of circles centred on F_0 with radii r_F given by:

$$r_F = SK_u^{1/\gamma} \quad (5)$$

The requirement that both ends of a duplex link need to be within their respective outage contours to be successful was not considered in [26]. Figure 3 illustrates this requirement if the interferer F_j interferes with both ends of the wanted link (e.g. F_j is a mobile–fixed station interferer pair approximating a point source with $P_u = P_d$ and $K = K_u = K_d$). The region of link closure, or cell, is the area of intersection between the two outage contours.

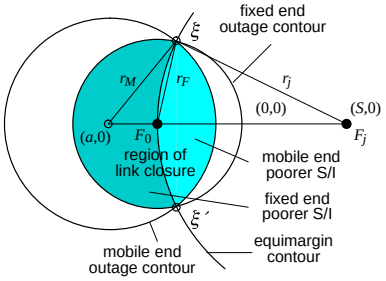

Figure 3 – Region of link closure

The equimargin contour (the contour where the link margin is the same at the fixed and mobile ends) can be shown to be a circle of radius S centred on the interferer F_j. The intersection of the two outage contours (denoted $\xi = (x,y)$ and $\xi' = (x,-y)$ in figure 3) necessa-

rily lies on the equimargin contour, and by solving equations (3) and (5), the points of intersection can be found to be given by:

$$\xi = \left(\frac{SK^{2/\gamma}}{2}, \pm SK^{1/\gamma} \sqrt{1 - \frac{K^{2/\gamma}}{4}} \right) \quad (6)$$

When $K^{2/\gamma} > 4$ (a weak interferer) the outage contours no longer intersect, whereupon the fixed end outage contour completely encloses the mobile end outage contour. The change in the cell shape as a function of K is illustrated in figure 4.

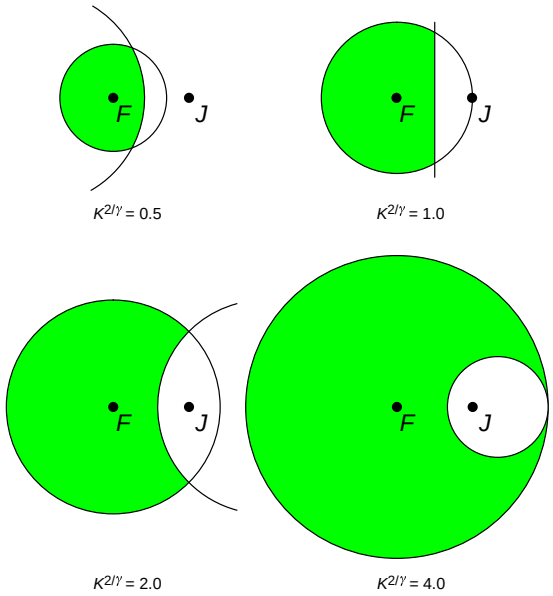

Figure 4 – Cell shape as a function of *K*

Two special values of K will now be defined. The first value, denoted K_e (for 'K enclosed') is that value of K at which the interferer is first enclosed by the mobile end outage contour. From examining figure 2 and equation (3) it is clear this value is given by:

$$K_e = 1 \quad (7)$$

which represents the pathological case of the interferer being enclosed by an outage contour of infinite radius. The second value, denoted K_c (for 'K critical') is that value of K at which the cell periphery first becomes entirely determined by outage conditions at the fixed end of the link, which occurs when the two outage contours intersect at a single point. If $K = K_u = K_d$, equation (6) applies, and hence a single point of intersection occurs at:

$$K_c = 2^{\gamma} \quad (8)$$

2.2 Single Interferer – Interference and Noise

The link outage model with a single interferer in [26] was based upon the assumption that there was no minimum received signal strength requirement in order for the link to close, i.e. receivers were noiseless.

A noisy receiver can be modelled as a noiseless receiver operating in the presence of two interference sources, one a source of ubiquitous noise power N and the other an interference source I. If these two sources are uncorrelated their powers add, and the requirement for link closure becomes $S/[N+I] \geq Z$ if the same protection ratio applies to noise and interference.

From first principles (following the interference scenario of figure 1) the outage contour at the *mobile* end of the link, in the presence of receiver noise, satisfies the expression:

$$R^{\gamma}_{0_M} = \frac{K_d R_j^{\gamma}}{1 + \frac{N}{\kappa P_d} R_j^{\gamma}} \quad (9)$$

R_j and R_0 are not independent, and it can be shown that this equation does not have a general functional solution for R_0 for all γ. Thus the outage contour at the mobile end in the presence of receiver noise is not a simple curve and is a 'higher plane curve' [27].

However, the outage contour at the *fixed* end of the link remains a family of circles centred on F_0 but of a smaller radius r_F compared to the noise–free case (c.f. equation (5)) as S and R_0 are independent:

$$R^{\gamma}_{0_F} = \frac{K_u S^{\gamma}}{1 + \frac{N}{\kappa P_u} S^{\gamma}} \quad (10)$$

If $K_u = K_d$ the equimargin contour remains a circle of radius S centred on the interferer, as in the noise–free case, because the addition of receiver noise equally affects both ends.

2.3 The Interference to Noise Ratio (INR)

In the mobile end outage equation (9) the term '1+ $N/(\kappa P_d R_j^{-\gamma})$' appears, and in the fixed end outage equation (10) the term '1+ $N/(\kappa P_u S^{-\gamma})$' appears. The second part of each of these terms is the receiver noise power N divided by the interference spill power from F_j received at the mobile station M_0 in the first case and at the fixed station F_0 in the second.

This term is dimensionless and is a measure of the extent of noise or interference dominance of the wanted link, and thus the extent to which the outage contours deviate from the noise–free case. This term (inverted) will be defined as the 'interference to noise ratio' or INR and given the symbol η. At the mobile end, the INR will be denoted η_M and is thus:

$$\eta_M = \frac{\kappa P_d R_j^{-\gamma}}{N} \tag{11}$$

whilst at the fixed end the INR will be denoted η_F and is thus:

$$\eta_F = \frac{\kappa P_u S^{-\gamma}}{N} \tag{12}$$

Thus equation (9) for the mobile end outage contour can be rewritten as:

$$R_{0_M}^{\gamma} = K_d R_j^{\gamma}\left[\frac{\eta_M}{\eta_M + 1}\right] = \psi\left[\frac{1}{\eta_M + 1}\right] \tag{13}$$

and equation (10) for the fixed end outage contour can be rewritten as:

$$R_{0_F}^{\gamma} = K_u S^{\gamma}\left[\frac{\eta_F}{\eta_F + 1}\right] = \psi\left[\frac{1}{\eta_F + 1}\right] \tag{14}$$

where the parameter ψ is a function of four basic system parameters ($\psi = \kappa P_t/ZN$).

By using η as a parameter, these equations provide a seamless description of the size and shape of the outage contours for all interference conditions from purely noise limited to purely interference limited conditions.

In the noise only case ($\eta = 0$) the mobile and fixed end outage contours are identical, i.e. a circle, centred on F_0, of a radius determined by the receiver noise level ($R_0 = \psi^{1/\gamma}$). In the interference only case ($\eta \to \infty$) the equations reduce to those in [26].

As both ends of the link must be above threshold for the link to close, an important result is that the range described by equation (14) represents the *maximum* range for M_0 regardless of the link conditions at the mobile end.

2.4 Outage Contour Families

The mobile end outage equation (13) can be rewritten in terms of η_F using the relationship $\eta_M = \eta_F(P_d/P_u)(S/R_j)^{\gamma}$:

$$R_{0_M}^{\gamma} = R_j^{\gamma}\left[K_d - R_{0_M}^{\gamma} P_u S^{-\gamma}/P_d \eta_F\right] \tag{15}$$

By solving equations (14) and (15) when $K = K_u = K_d$, the coordinates ξ of the intersection of the two outage contours can be shown to be:

$$\xi_x = \frac{S}{2}\left[\frac{K\eta_F}{\eta_F + 1}\right]^{2/\gamma} \tag{16}$$

$$\xi_y = \pm\, S\left[\frac{K\eta_F}{\eta_F + 1}\right]^{1/\gamma} \sqrt{1 - \frac{1}{4}\left[\frac{K\eta_F}{\eta_F + 1}\right]^{2/\gamma}} \tag{17}$$

Although more problematic, the expressions for K_e and K_c in the presence of receiver noise can also be derived. It can be shown that:

$$K_e = \frac{1}{\eta_F}\left[1 + \eta_F^{1/(\gamma+1)}\right]^{\gamma+1} \tag{18}$$

$$K_c = 2^{\gamma}\left[\frac{\eta_F + 1}{\eta_F}\right] \tag{19}$$

which reduce to equations (7) and (8) respectively in the noise free case (i.e. when $\eta_F \to \infty$). $K_c > K_e$ for all η_F, except when $\eta_F = 1$ whereupon $K_c = K_e = 2^{\gamma+1}$.

The fixed and mobile end outage contours (as per equations (14) and (15) respectively) were plotted for a range of K and for η_F of 0.1, 1.0, 10.0 and 100.0 and $\gamma = 2$ (figures 5 to 8).

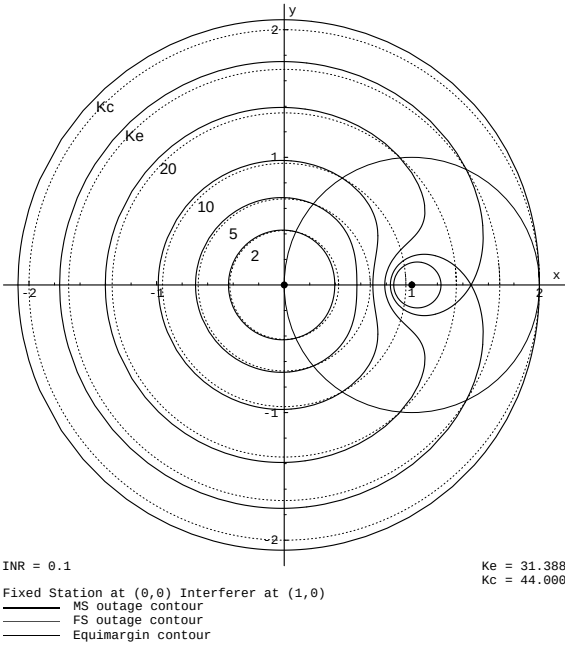

Figure 5 – Outage contours for η_F = 0.1 and γ = 2

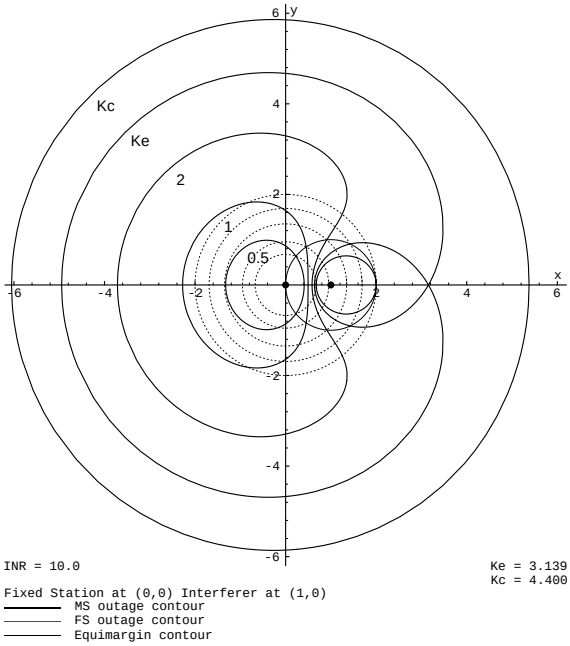

Figure 7 – Outage contours for η_F = 10.0 and γ = 2

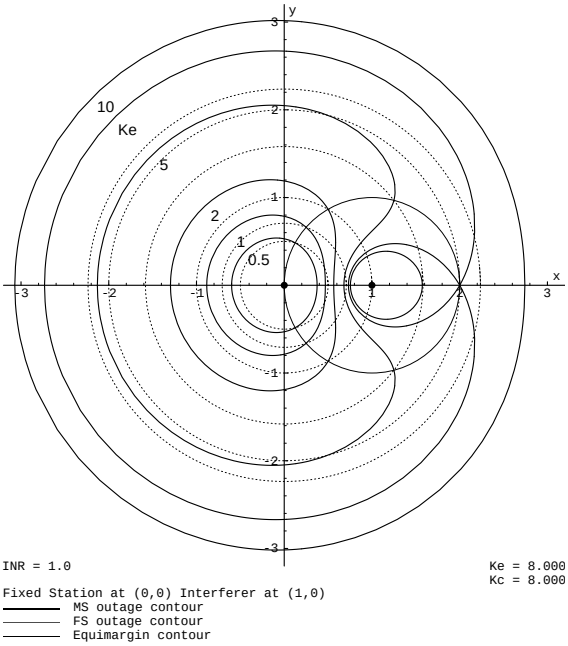

Figure 6 – Outage contours for η_F = 1.0 and γ = 2

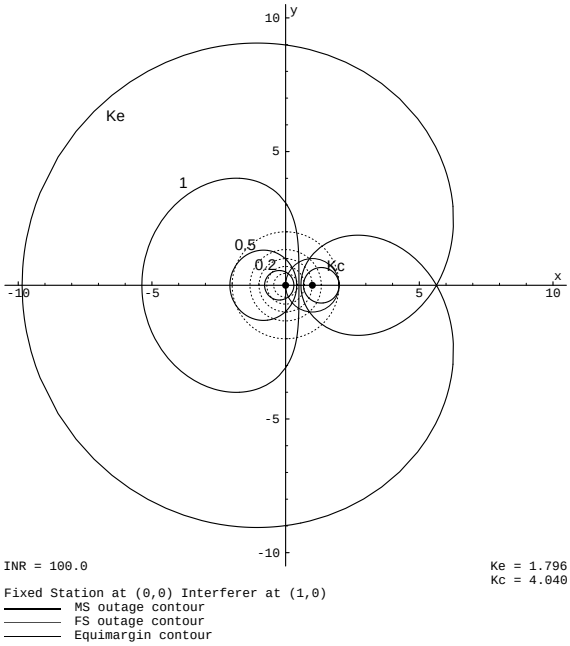

Figure 8 – Outage contours for η_F = 100 and γ = 2. The outer part of the K_c contour is not shown.

A number of comments may be made about the resultant outage contours:

- When the INR is small (i.e. $\eta_F < 0.1$), the system is noise dominated. The outage contours at both ends of the link are approximately circles, centred on the fixed station, at a radius determined by the receiver noise level. Only near the interferer does the mobile end outage contour deviate.
- When the INR is large (i.e. $\eta_F > 10.0$), the system is interference dominated. Under these conditions, the fixed end outage contours are much smaller in radius than the mobile end outage contours.
- When the interferer and noise powers are comparable in magnitude (i.e. $0.1 < \eta_F < 10.0$) the mobile end outage contour behaviour is strongly influenced by both the interferer and the receiver noise.
- The equimargin contour (necessarily) still passes through the intersection of the fixed and mobile end outage contours for all values of η_F and K.
- At $K = K_e$, the mobile end outage contour exhibits a property where it forms a Limaçon–like curve. However, no Limaçon can be made to match it exactly [27].

3 Simulation of Mobile Systems

What values of K and η might be experienced in typical cellular and microcellular systems? Consider a cochannel interferer pair where the spill power P_d into the wanted downlink and P_u into the wanted uplink is equal to the mobile terminal's transmitter power P_t. In an AMPS system with a cluster size of 7, a cochannel interferer is on average 4.6 cell radii distant from the fixed station under consideration [5].

If a S/[N+I] ratio of 18 dB is required for the wanted link, then $K = P_t/ZP_d = 1/Z = 0.016$. Assuming a transportable transmitting at 1 W, and a small cell radius of 1 km, the interference power received at the central fixed station from a single cochannel interferer at a distance of 4.6 km in a $\gamma = 3$ environment is approximately –111 dBm. This is approximately equal to the noise floor of a receiver in a typical mobile terminal, so $\eta_F \approx 1.0$.

Using equations (14) and (15), the fixed and mobile end outage contours for this AMPS scenario may be computed and they are shown in figure 9. The resultant cell is the region of intersection between the two outage contours.

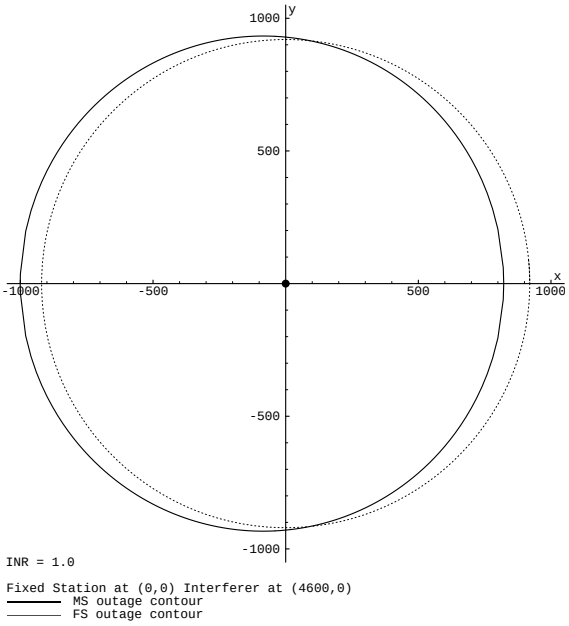

Figure 9 – Mobile and Fixed end outage contours for an AMPS cell (η = 1.0, K = 0.016, γ = 3)

Using a computer model, the above analytical result can be checked numerically. Figure 10 below shows a 3–dimensional representation of the resultant AMPS cell, showing the link S/[N+I] (z–axis) available to a mobile communicating with the base station at the origin.

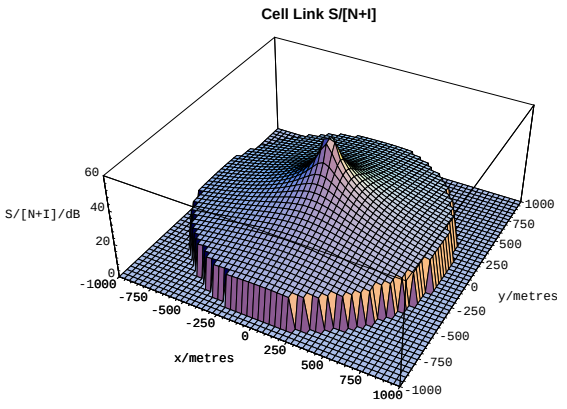

Figure 10 – 3D plot of AMPS cell

Figure 11 is the 'critical link end' plot, which shows which end of the link has the poorer S/[N+I] (i.e. which end fails first). The equimargin contour is the boundary between these

two regions and is as predicted – a circle of radius 4.6 km centred on the interferer.

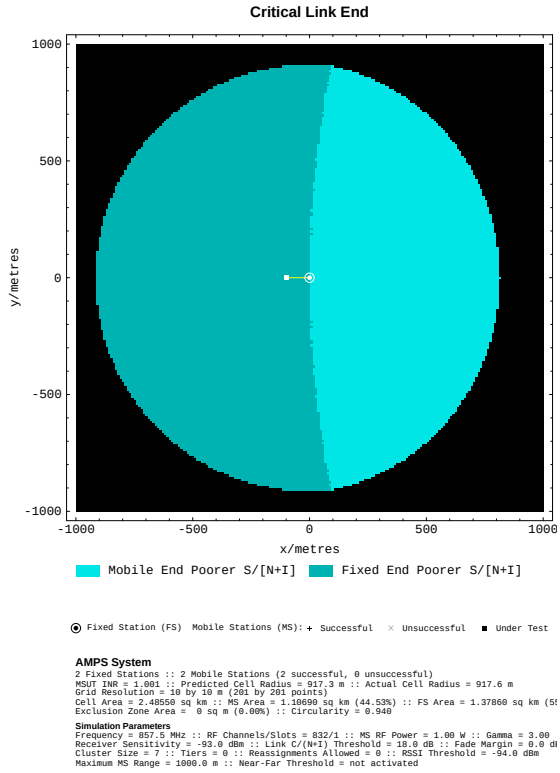

Figure 11 – AMPS cell Critical Link End plot

Figures 9 to 11 show that even with a small AMPS cell, a cochannel interferer causes little difference between the mobile and fixed end outage contours – they are nearly circular and coincident. Thus the resultant cell is also nearly circular. This is consistent with the assumption that in large cell systems a regular cell shape results when uniform propagation conditions are assumed. However, what happens in a microcellular system?

Consider a DECT system with an *effective* cluster size of 3 (i.e. a cochannel interferer, on average, appears 3 cell radii distant from the base station under consideration). If a S/I ratio of 9 dB is required for a wanted link, then $K = P_t/ZP_d = 1/Z = 0.126$. Assuming a portable transmitting at 250 mW, and a small *intended* cell radius of 100 m, the interference power received at the central fixed station from a single cochannel interferer pair at a distance of 300 m in a $\gamma = 3$ environment is approximately –88 dBm. This is very much larger than the noise floor of a receiver in a typical mobile terminal, giving $\eta_F \approx 200$.

Using equations (14) and (15), the outage contours for this DECT scenario may be computed and they are shown in figure 12. The mobile end outage contour is now greatly offset from the central fixed station as predicted by equation (15).

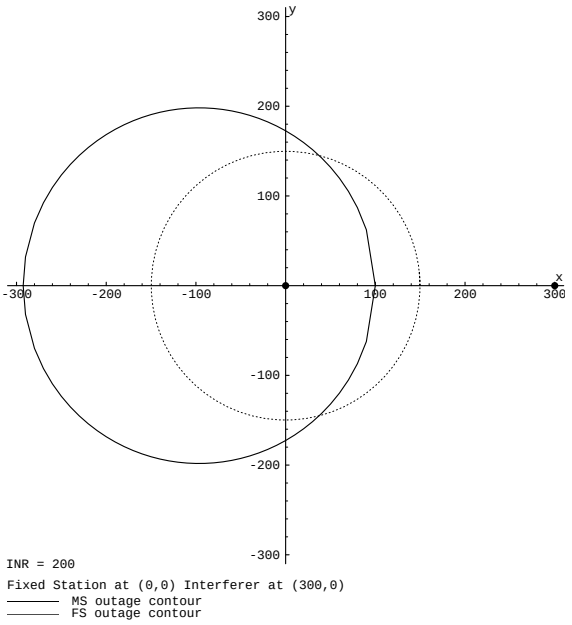

Figure 12 – Mobile and Fixed end outage contours for a DECT cell (η = 200, K = 0.126, γ = 3)

The analytical result was checked numerically, figure 13 showing the 3–dimensional representation of the resultant DECT cell, and figure 14 showing critical link end plot.

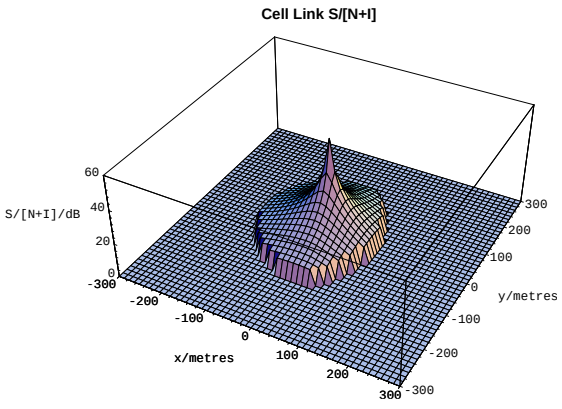

Figure 13 – 3D plot of DECT cell

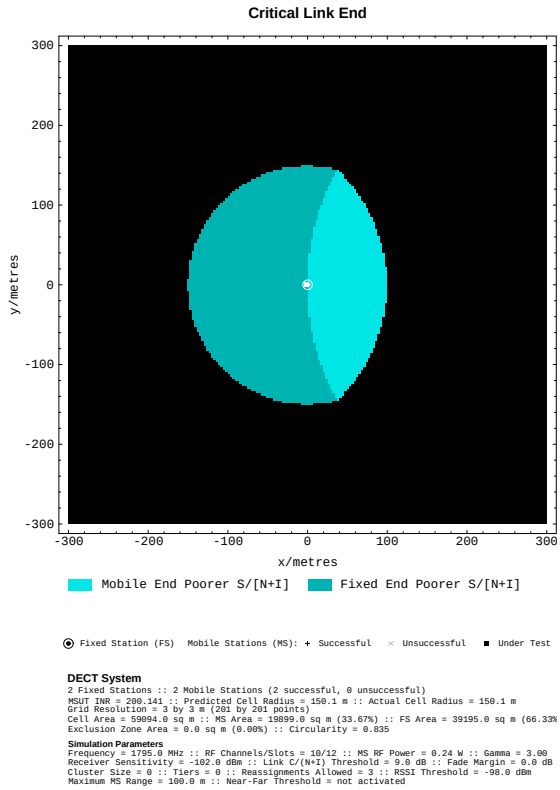

Figure 14 – DECT cell Critical Link End plot

It can be seen from figures 12 to 14 that the DECT microcell is no longer circular. Furthermore, its size will be now much more sensitive to the interference level.

Equation (14) indicated that the maximum cell size for a particular mobile is a constant multiplied by $1/(\eta_F+1)$. For large values of η_F, $1/(\eta_F+1) \approx 1/\eta_F$ and thus the cell size is very sensitive to η_F, and by extension, the arrangement of interferers. For the above DECT cell, η_F was quite large at approximately 200.

In contrast, with the smaller values of η_F as might be experienced in a large cell system (as in the earlier AMPS example), $1/(\eta_F+1) \approx 1$ and the cell size is relatively independent of the interferers.

Hence, there seems to be a significant difference between the cochannel interference conditions experienced in large cell systems and microcellular systems. This difference results in different properties in the outage contours and different sensitivities in the resultant cell size to the location of the cochannel interferer.

These results suggest that contiguous cell coverage will be much harder to achieve in a microcell system than in a large cell system as a microcell system is more likely to be interference limited [14]. This could have severe ramifications for the offered service quality and handoff reliability.

4 Conclusion

Outage contours and cell sizes experienced by individual mobile stations in a cellular or microcellular system can be modelled as a function of the ratio of the interference power to the noise power at the receiver, a ratio denoted the interference to noise ratio or INR.

Preliminary results suggest that microcellular systems are more interference limited (i.e. have a larger INR) than large cell systems, and will experience larger variation in cell sizes.

This suggests that a system wide microcellular design methodology will need to address the statistics of the INR if contiguous radio coverage is required for a certain proportion of mobile stations.

5 References

[1] W.R. Young: “Advanced Mobile Phone Service: Introduction, Background and Objectives”, *Bell System Technical Journal*, vol 58 no 1 pp 1–14, Jan 1979.

[2] V.H. MacDonald: “The Cellular Concept”, *Bell System Technical Journal*, vol 58 no 1 pp 15–41, Jan 1979.

[3] W.C.Y. Lee: “Smaller Cells for Greater Performance”, *IEEE Communications Magazine*, vol 29 no 11 pp 19–23, Nov 1991.

[4] W.C.Y. Lee: “Quality and Capacity in Cellular”, *Electro International Conference Record*, pp 519–20, New York, USA, 16–18 Apr 1991.

[5] W.C.Y. Lee: “Spectrum Efficiency in Cellular”, *IEEE Transactions on Vehicular Technology*, vol 38 no 2 pp 69–75, May 1989.

[6] W.C.Y. Lee: “Estimate of Channel Capacity in Rayleigh Fading Environment”, *IEEE Transactions on Vehicular Technology*, vol 39 no 3 pp 187–189, Aug 1990.

[7] D.C. Cox: “Wireless Network Access for Personal Communications”, *IEEE Communications Magazine*, pp 96–115, Dec 1992.

[8] J.G. Gardiner: “Second Generation Cordless (CT2) Telephony in the UK: Telepoint Services and the common air interface”, *Electronics and Communication Engineering Journal*, pp 71–78, April 1990.

[9] J. Sarnecki, C. Vinodrai, A. Javed, P. O’Kelly, K. Dick: “Microcell Design Principles”, *IEEE Communications Magazine*, vol 31 no 4 pp 76–82, April 1993.

[10] T.S. Rappaport: “Wireless Personal Communications: Trends and Challenges”, *IEEE Antennas and Propagation Magazine*, vol 33 no 5 pp 19–29, Oct 1991.

[11] A. Gamst, “Remarks on Radio Network Planning”, *Proceedings of the 37th IEEE Vehicular Technology Conference*, p. 164, Tampa, 1–3 June 1987.

[12] I. Goetz: “Transmission Planning for Mobile Telecommunication Systems”, *6th IEE International Conference on Mobile Radio and Personal Communications*, pp 126–130, Coventry, UK, 9–11 Dec 1991.

[13] W.T. Webb: “Modulation Methods for PCNs”, *IEEE Communications Magazine*, vol 30 no 12 pp 90–95, Dec 1992.

[14] D. Everitt, D. Manfield: “Performance Analysis of Cellular Mobile Communications Systems with Dynamic Channel Assignment”, *IEEE Journal on Selected Areas of Communications*, vol 7 no 8 pp 1172–1180, Oct 1989.

[15] P.T.H. Chan, M. Palaniswami and D. Everitt: “Dynamic Channel Assignment for Cellular Mobile Radio System using Self–Organising Neural Networks”, *6th Australian Teletraffic Research Seminar*, pp 89–95, Wollongong, Australia, 28–29 Nov 1991.

[16] S–W. Wang, S.S. Rappaport: “Signal to Interference Calculations for Corner Excited Cellular Communications Systems”, *IEEE Transactions on Communications*, vol 39 no 12 pp 1886–1896, Dec 1991.

[17] S.W. Wang, S.S Rappaport: “Signal to Interference Calculations for Balanced Channel Assignment Patterns in Cellular Communications Systems”, *IEEE Transactions on Communications*, vol 37 no 10 pp 1077–1087, Oct 1989.

[18] J.P. Driscoll: “Relevance of Receiver Filter Performance and Operating Range for CT2/CAI Telepoint Systems”, *Electronics Letters*, vol 28 no 13 pp 1200–1201, 18 June 1992.

[19] J.P. Driscoll: “Some Factors Which Affect the Traffic Capacity of a Small Telepoint Network”, *5th IEE International Conference on Mobile Radio and Personal Communications*, pp 167–71, Coventry, UK, 11–14 Dec 1989.

[20] A.O. Fapojuwo, A. McGirr, S. Kazeminejad: “A Simulation Study of Speech Traffic Capacity in Digital Cordless Telecommunications Systems”, *IEEE Transactions on Vehicular Technology*, vol 41 no 1 pp 6–16, Feb 1992.

[21] P.A. Ramsdale, A.D. Hadden, P.S. Gaskell: “DCS1800 – The Standard for PCN”, *6th IEE International Conference on Mobile Radio and Personal Communications*, pp 175–179, Coventry, UK, 9–11 Dec 1991.

[22] S. Sato, K. Takeo, M. Nishino, Y. Amezawa, T. Suzuki: “A Performance Analysis on Non-uniform Traffic in Microcell Systems”, *IEEE International Conference on Communications* (ICC 93), vol 3 pp 1960–1964, Geneva, Switzerland, 23–26 May 1993.

[23] S.T.S. Chia: “The Universal Mobile Telecommunication System”, *IEEE Communications Magazine*, vol 30 no 12 pp 54–62, Dec 1992.

[24] S.T.S. Chia: “Providing Ubiquitous Cellular Coverage for a Dense Urban Environment”, *44th Vehicular Technology Conference*, pp 1045–1049, Stockholm, Sweden, 8–10 Jun 1994.

[25] A. Kegel, W. Hollemans, R. Prasad: “Performance Analysis of Interference and Noise Limited Cellular Land Mobile Radio”, *41st IEEE Vehicular Technology Conference*, pp 817–821, St Louis, USA, 19–22 May 1991.

[26] C.E. Cook: “Modelling Interference Effects for Land Mobile and Air Mobile Communications”, *IEEE Transactions on Communications*, vol 35 no 2 pp 151–165, Feb 1987.

[27] E.H. Lockwood: *A Book Of Curves*, Cambridge University Press, England, 1967.